JOURNAL OF MATERIALS SCIENCE 24 (1989) 3300–3304

Formation of willemite from powder mixture with TiO_2 addition

C. C. LEE, P. SHEN
Institute of Materials Science and Engineering, National Sun Yat-Sen University, Kaohsiung, Taiwan

H. Y. LU
Materials Research Laboratories, Industrial Technology Research Institute, Chutung 31015, Taiwan

The formation of willemite, Zn_2SiO_4, from stoichiometric oxide powder mixtures either with 3.2 mol% TiO_2 additive (ZST) or without TiO_2 addition (ZS) and from flux-added glaze powder (G) were studied in the temperature range of 650 to 1515° C. Activation energy of willemite formation were 167, 226 and 188 kJ mol^{-1} for G, ZS and ZST specimens respectively. TiO_2 addition not only reduced the activation energy of willemite formation, but was also found to stabilize the metastable phase, β-Zn_2SiO_4, to room temperature after cooling from melts. Annealing of the melted ZnO–SiO_2–TiO_2 composition resulted in the transformation of β-Zn_2SiO_4 to α-Zn_2SiO_4. It is suggested that the substitution of a Si^{+4}-site by a Ti^{+4} ion contributes to the stabilization of the β-phase, the larger d-spacing, and smaller c/a ratio of willemite transformed.

1. Introduction

Willemite is α-Zn_2SiO_4 with a phenacite structure and belongs to the orthosilicates [1]. Besides occurring as a natural mineral, willemite is also an important crystalline phase in glaze [2] and in glass ceramics [3]. Willemite appears to be the sole thermodynamically stable binary compound at temperatures between 800° C and the liquidus according to the atmospheric phase diagram of the ZnO–SiO_2 system [4]. Five polymorphs of Zn_2SiO_4 (I–V) including willemite (I) have been found to be stable at various temperature and pressure conditions [5, 6]. The existence of metastable β- and γ-Zn_2SiO_4 at atmospheric pressure has been suggested by X-ray diffraction study [7]. The beta phase has subsequently been obtained by other investigators as a result of heating ZnO–SiO_2 [8] or ZnO–MnO–SiO_2 [9] mixtures as well as from the dehydration of hemimorphite [10]. According to Taylor [10] the beta–alpha transition is an oriented one and involves little density change. The devitrification of zinc silicate glasses also yield these metastable phases [8] because they represent less atomic rearrangement than willemite necessary for the glass to crystallize [8]. In ZnO–Al_2O_3–SiO_2 glasses, the initial phase developed between 800 and 950° C upon ageing has a stuffed keatite structure which transforms irreversibly into willemite at about 980° C [11]. According to the same authors [11], addition of metal oxides caused marked changes in the crystal growth rate of stuffed keatite, although the activation energy of crystal growth was changed little; similarly the minor additions of various metal oxides influenced the crystal growth rate but did not influence the crystal structure to any great extent.

As well as in many other glass ceramics, titanium dioxide has been used as nucleating agent in the ZnO–Al_2O_3–SiO_2 system because of its coordination effect [12] and the inclusion of alkali and alkali earth oxides significantly modifies the crystallization behaviour. Information on physical, chemical and themodynamic properties of titanium-bearing silicate melts generally is consistent with a polymerizing role of Ti^{+4} in the melts [13]. The growth kinetics of crystals in glass ceramics of a number of composition systems have been studied, however little is known about the reaction kinetics of constituent oxides in the ZnO–SiO_2–TiO_2 system. In a similar way to the ZnO–SiO_2 binary system, ZnO and TiO_2 have an affinity for each other and tend to combine to form Zn_2TiO_4 or $ZnTiO_3$ [14–16]. A process to minimize sintering but to promote the formation of pigment size (submicrometer to 5 μm) Zn_2TiO_4 powder from zinc and titanium-source precursors has been suggested [16].

In the present study the DTA (up to 1100° C) and powder X-ray diffraction of the specimens fired in the temperature range of 650 to 1515° C from the compositions of the ZnO–SiO_2–TiO_2 system, as well as the flux-added glaze system, were conducted to investigate the reaction kinetics of willemite from constituent oxide powders.

2. Experimental procedures

Commercial glaze powder (G) of compositions of ZnO (28.34), SiO_2 (51.22), TiO_2 (4.07), Na_2O (5.36), CaO (4.06), FeO (3.34), K_2O (2.51) and Al_2O_3 (1.10) in molar ratios was donated by Mr Chau Sun of Tien-Shin Kiln*. The G powder was oven dried at

*Mr Chau Sun, formerly with the National Palace Museum, a renowned pottery artist in Taiwan first suggested this research to us.

0022–2461/89 $03.00 + .12

TABLE I Phases identification (powder X-ray diffraction, Cuk_α) of G, ZS and ZST specimens sintered and cooled under various conditions

Sample	T(°C)	t(h)	Cooling	Phases present*
G1	–	–	–	z + aq
G2	650	24	furnace	z + aq
G3	700	16	water	z + bq + w
G4	750	16	furnace	z + aq + w
G5	750	16	water	z + bq + w
G6	900	1	furnace	z + aq + w
G7	900	1	water	z + bq + w
G8	1100	4	water	w
ZS1	–	–	–	z + aq
ZS2	800	72	furnace	z + aq
ZS3	900	24	water	z + bq + w
ZS4	1100	16	furnace	z + aq + w
ZS5	1100	16	water	z + bq + w
ZS6	1515	4	furnace	w
ZS7	1515	4	water	β-Zn_2SiO_4
ZS8	→1100**	→4**	→furnace**	w
ZST1	–	–	–	z + aq + r
ZST2	800	72	furnace	z + aq + zto
ZST3	850	72	water	z + bq + w + zto
ZST4	1100	16	furnace	z + aq + w + zto
ZST5	1100	16	water	z + bq + w + zto
ZST6	1515	4	furnace	β-Zn_2SiO_4 + trace zto
ZST7	1515	4	water	β-Zn_2SiO_4 + trace zto
ZST8	→1100**	→4**	→furnace**	w

*z: zincite, aq: α-quartz, bq: β-quartz, w: willemite, r: rutile, zto: zinc titanium oxide (α-Zn_2TiO_4)
**→denotes further heating of specimens water-quenched from 1515° C

110° C before being crushed to enable it to pass through a 63.5 μm sieve. Compositions designated as ZS and ZST were also prepared from the analytical reagent grade (Merck, FRG) powder of ZnO, SiO_2 and TiO_2. The ZnO powder was previously dissolved in glacial acetic acid to form a suspension. It was then added with half molar ratios of SiO_2 powder and stirred vigorously at 200° C to prepare ZS slurry. The ZS slurry was converted to zincite and α-quartz by calcination at 500° C. TiO_2 of 3.2 mol % when required, was added to the ZS slurry and calcined at 500° C to form ZST powder. The G, ZS, and ZST powders were die-pressed at 40 MPa to 10 mm diameter discs. Sample discs were sintered in an open-air furnace and followed by either water quenching or furnace cooling. Typical conditions used in heating and cooling runs are given in Table I. The isothermal treatments for various periods of time followed by water-quenching were also conducted at 700, 750, 775 and 800° C for the G specimen and at 1000, 1050, 1075 and 1100° C for both the ZS and ZST specimens for kinetics study.

Sintered discs were ground to powder by using an agate mortar and pestle. Crystalline phases were identified by using Cuk_α radiation operating at 40 kV, 25 mA. Reaction kinetic data were accumulated by integrating the willemite {1 4 0} peak area for each willemite-bearing specimen. The fraction of reaction at any time, t, was calculated by comparing the {1 4 0} peak areas of the sample containing 100% willemite to that of the partially reacted sample; i.e. fraction of reaction $x = A_t/A_{100\%\ \text{willemite}}$. Peak areas of willemite {1 1 3} and {2 2 0} were also measured to eliminate the preferred orientation effect. DTA runs were made on a Shimazu Thermal Analyser DT-30. 30 mg samples were heated at a rate of 2° C min^{-1} with alumina as a reference material.

Thin sections 30 μm in thickness, initially for plane polarized microscopy and finally for scanning electron microscopy (SEM, JEOL, JSM 35-CF, operating at 25 kV) were prepared from the sintered discs. SEM coupled with energy dispersive X-ray (EDX) analysis was used to characterize the qualitative composition of the gold-coated thin sections.

3. Results

3.1. Phase identification

According to X-ray diffraction, the as-received glaze (G) contained zincite (ZnO) and α-quartz (G1 in Table I). The willemite phase started to appear when fired at 700° C and the amount of willemite increased when the temperature was raised. The G sample heated at 1100° C contained predominantly willemite (G8, Table I). Water quenching from 750° C (G5) and 900° C (G7) produced β-quartz instead of α-quartz which was formed by furnace cooling.

Crystalline phases resulting from firing the ZS powder mixture below 800° C were again unreacted zincite and quartz (Table I). Willemite appears at 900° C and its amount increased when the temperature was raised. The type of quartz obtained, α- or β-quartz, was also dependent on the cooling rate (ZS4, ZS5). Water quenching of the melted ZS mixture in a pure alumina (~99.8%) crucible at 1515° C resulted in the β-Zn_2SiO_4 phase (ZS7) instead of α-Zn_2SiO_4 in furnace-cooled ZS sample. Further heating of the quenched ZS7 sample at 1100° C, however, yielded the willemite phase (ZS8). On the other hand, heating the ZS powder mixture at 1100° C followed by either furnace-cooling (ZS4) or water-quenching (ZS5) gave α-Zn_2SiO_4 besides unreacted oxides.

The temperature at which willemite was found was reduced from 900 to 850° C (ZST3) when TiO_2 was added to ZS powder (Table I). The α-Zn_2TiO_4 phase also appeared before willemite emerged in sample heat-treated at 800° C; its presence persisted in all samples but one (ZST8) in this series. Apart from α- and β-quartz polymorph, samples heated at 1100° C for 16 h followed by water-quenching or furnace-cooling did not produce any discernible difference in XRD patterns (ZST4, ZST5). The predominant phase, β-Zn_2SiO_4, and trace Zn_2TiO_4 were obtained both by furnace-cooling and water-quenching (ZST6, ZST7) after the powder mixture was heated to melt at 1515° C. Further heating of these samples at 1100° C resulted in the formation of willemite at the expense of β-Zn_2SiO_4 and Zn_2TiO_4. A larger d-spacing and a smaller c/a ratio were found for the willemite phase in sample ZST8 comparing to that in sample ZS8 (Table II). The β-Zn_2SiO_4 also has larger d-spacings in ZST than in ZS specimens (Table II), and the β-Zn_2SiO_4 crystallized from ZST melts has larger d-spacing via furnace-cooling (ZST6) than water-quenching (ZST7). Step scanning on the {h k l}'s of willemite or β-Zn_2SiO_4 also confirmed the shifting of d-spacings in various ZS and ZST specimens.

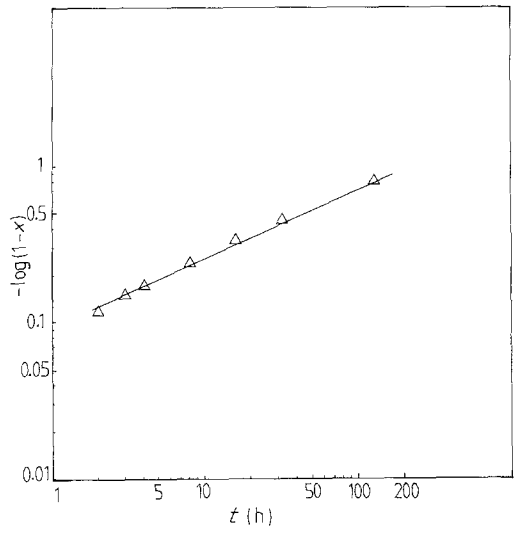

Figure 1 JMA plot of G specimens fired at 700° C.

3.2. Reaction kinetics

X-ray diffraction traces from G samples heated at 700° C for various periods of time followed by water-quenching, were taken to investigate the reaction kinetics. Reaction kinetics based on the willemite phase obtained can be approximated to the general Johnson–Mehl–Avrami (JMA) equation [17–20]

$$x = 1 - \exp(-kt^n) \quad (1)$$

where x is fraction reacted, t is reaction time. The double-log JMA plot of $-\log(1-x)$ against t shown in Fig. 1 gave a straight line of slope 0.45.

Arrhenius plot was constructed for estimating the activation energy of willemite formation. Plotting the time required for the reaction to reach 50% ($t_{0.5}$) plotted against ($1/T$) on the semi-log scale, for G samples heated at T = 700 to 800° C, the activation energy was determined as ~ 167 kJ mol^{-1} (Fig. 2).

The ZS and ZST samples fired at 1100° C followed by water-quenching were examined for the willemite phase content. The rate of willemite formation was faster for the TiO_2-added ZST sample. Reaction kinetics can also be approximated to the general equation of Equation 1 as has been described, and the double-log plot (Fig. 3) yielded two parallel lines of slope of ~ 0.50. The activation energies of willemite formation determined for T = 1000 to 1100° C, were ~ 226 kJ mol^{-1} and 188 kJ mol^{-1} for ZS and ZST samples, respectively (Fig. 4).

3.3. DTA and EDX analysis

An endothermic peak appeared at ~ 585° C for G, ZS and ZST samples (Figs 5a, b and c) which was due to the α–β quartz transformation. Melting occurred at 680° C for the G specimen as indicated by the slope changing of the DTA trace (Fig. 5a). No peak of willemite formation can be differentiated from the DTA curves for G, ZS, and ZST samples. However, an exothermic reaction covering a rather wide range of temperature was recognized; e.g. 850 to 900° C for G sample (Fig. 5a) and 700 to 950° C for ZST sample (Fig. 5c).

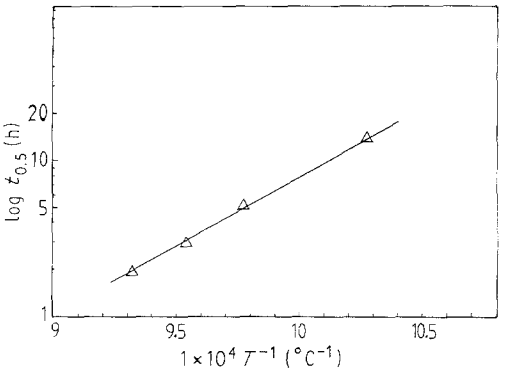

Figure 2 Arrhenius plot, ln ($t_{0.5}$) against $1/T$, of G specimens.

Needle-shape willemite crystals in a glass matrix, clustered to bundles were observed in the melted G sample by polarized microscopy. The ratio of atomic concentration was assumed to be proportional to the integrated counts ratio of silicon and zinc in EDX analysis and the proportionality constant, k, was determined from a stoichiometric willemite sample. Willemite crystals of c_{Si}/c_{Zn} ~ 0.54 in the G, ZS and ZST samples, were approximately stoichiometric in composition. Although a slight dissolution of iron in willemite of the G sample cannot be excluded as suggested by a few wt % solubility of iron in willemite mineral. A ratio of ~ 6.15 for the glass matrix of G sample indicated its silicon-rich nature.

4. Discussion

4.1. Willemite formation

In the system Na_2O–ZnO–SiO_2, the lowest eutectic temperature appears at ~ 680° C according to the phase diagram [21]. For the G sample, an endothermic reaction due to the eutectic melting was indicated by the slope changing of the DTA curve at 680° C (Fig. 5a). This explained the significant formation of willemite at ~ 700° C (Table I). For ZS and ZST samples, however, willemite did not appear significantly until the temperature was raised to ~ 900° C. It is likely that the liquid phase provided a faster path for

TABLE II d-spacings (nm) of willemite and β-Zn_2SiO_4 (b)

Sample	$(2\,2\,0)_w$	$(1\,1\,3)_w$	$(1\,4\,0)_w$	$(c/a)_w^*$	$(1\,0\,2)_b$	$(0\,1\,4)_b$	$(0\,3\,\bar{1})_b$
ZS4	0.3490	0.2837	0.2634	0.667	–	–	–
ZS7	–	–	–	–	0.3664	0.3520	0.2853
ZS8	0.3492	0.2836	0.2637	0.668	–	–	–
ZST4	0.3489	0.2837	0.2635	0.667	–	–	–
ZST6	–	–	–	–	0.3695	0.3561	0.2882
ZST7	–	–	–	–	0.3690	0.3554	0.2878
ZST8	0.3520	0.2856	0.2655	0.665	–	–	–

*ratio of lattice parameters along c and a-axis of willemite

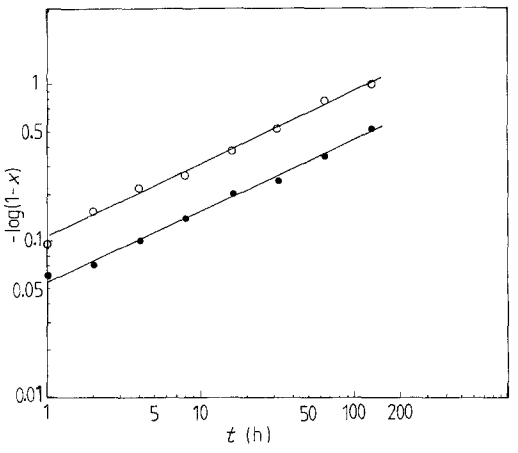

Figure 3 JMA plot of ZS (●) and ZST (○) specimens fired at 1100° C.

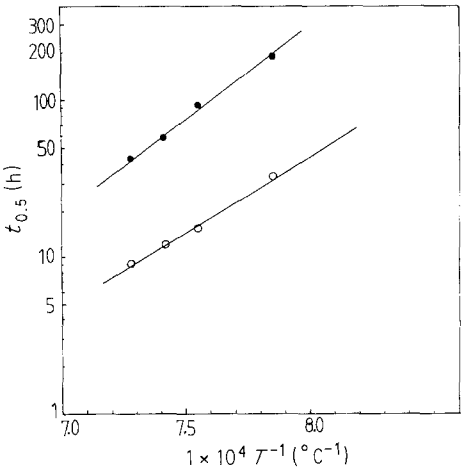

Figure 4 Arrhenius plots of ZS (●) and ZST (○) specimens.

matter transport to the reaction sites in G samples above 680° C. For ZS and ZST samples, however, melting did not occur except at 1515° C, therefore matter transport via the solid-state or vapour phase required a higher temperature for willemite formation.

Since water-quenching produced a similar amount of willemite as furnace-cooling for the G, ZS, and ZST samples, it appeared that the formation of willemite crystal occurred during heating rather than cooling from 1100° C. In contrast to furnace-cooling, water-quenching from ZS and ZST melts at 1515° C retained the β-Zn_2SiO_4 phase metastably; it followed that β-α Zn_2SiO_4 transformation occurred by furnace-cooling from 1515° C.

The β-Zn_2SiO_4 phase has been found in crystallized melt and glass [8]; an attempt to prepare this phase by direct solid-state reaction was unsuccessful [8]. According to Taylor [10], the structure of β-Zn_2SiO_4 was derived from a distorted tridymite- or cristobalite-like framework in which half of the silicon was replaced by zinc and additional zinc atoms introduced into suitable interstices. Thus, it was suggested that β-Zn_2SiO_4 appear prior to the equilibrium phase (α-Zn_2SiO_4) because minimum atomic rearrangement was necessary for the glass to crystallize as β-Zn_2SiO_4. During cooling from the melt or heat treatment of supercooled glass, the β-phase then converted to willemite by polymerization of ZnO_4-tetrahedra to SiO_4-tetrahedra to form phenacite group phase, willemite.

4.2. Effect of TiO_2 addition

The effect of TiO_2-addition was not significant for firings at temperatures lower than 1100° C, except that trace Zn_2TiO_4 was found in ZST samples. The broad exothermic peak observed at ~ 800° C (Fig. 5c) can be attributed to the Zn_2TiO_4 formation. However for heat treatment at 1515° C, TiO_2 addition was found to retain the metastable β-Zn_2SiO_4 even when samples were furnace-cooled. It appeared that the dissolution of TiO_2 enabled metastable β-Zn_2SiO_4 to be retained, although β-Zn_2SiO_4 was not stable when subjected to further heating at 1100° C. The larger d-spacings of β-Zn_2SiO_4 obtained in ZST samples (Table II), compared with those of ZS samples also suggests a possible substitution of Si^{+4} (0.039 nm) by the larger Ti^{+4} ion (0.064 nm) [22] in tetrahedral network position of β-Zn_2SiO_4 and possibly in silicate melts [13]. Spectroscopic information on the structural role of Ti^{+4} in silicate melts suggested that Ti^{+4} most often occurred in tetrahedral coordination, although octahedral exceptions were found in titanium-rich silica melts and in silica-free titanate melts [13]. On the basis of the oriented transition of β–α Zn_2SiO_4, Taylor [10] suggested that the tetrahedral framework in β-Zn_2SiO_4 resembles the distorted one of $BaAl_2O_4$ except that the tetrahedral zinc in the framework caused further distortion and hence reduction in the size of the interstices. Since Ti^{+4} readily adopted tetrahedral coordination in silicate melts [13], it can be assumed that

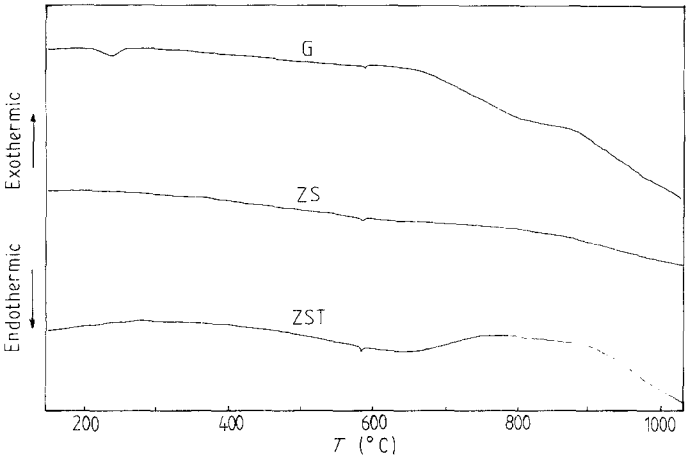

Figure 5 DTA traces of G, ZS and ZST specimens.

the presence of tetrahedral Ti^{+4} in the framework of melts or β-Zn_2SiO_4 caused further distortion which again reduced the size of the interstices to accommodate an atom as small as zinc (Zn^{+2} = 0.083 nm). By analogy with $BaAl_2O_4$ and other structurally similar compounds, zinc was probably octahedrally rather than tetrahedrally coordinated in the interstices. This might explain the relative low stability of β- relative to α-Zn_2SiO_4 in which all of the zinc is tetrahedrally coordinated. Further heating at 1100° C resulted in the disappearance of trace Zn_2TiO_4, and the transformation of β-Zn_2SiO_4 to willemite of larger d-spacings due to the incorporation of Ti^{+4} in the lattice.

4.3. Reaction kinetics

For ZS and ZST samples, $n \sim 0.5$ in Equation 1 represents a parabolic reaction kinetics, and the reaction was diffusion-limited [23]. Willemite was formed predominantly by reaction of ZnO and SiO_2 powder in the present study. Solid-state reaction occurred amongst the contact areas of powder particles in the mixture below 1100° C and resulted in a layer of products, i.e. willemite. Diffusion of reactants through this progressively growing layer was necessary for further reaction to proceed. Addition of TiO_2 did not alter the parabolic reaction kinetics. However, the activation energy of willemite formation was reduced significantly from 226 to 188 kJ mol^{-1}. Furthermore, the reaction rate was also increased while the willemite formation temperature was reduced to 850 from 900° C. This implied that, although the actual reaction rate was enhanced by TiO_2, the diffusion of Zn^{+2} and Si^{+4} to the product sites still governed the reaction kinetics. It is, therefore, suggested that TiO_2 acts as a catalyst in the SiO_2–ZnO reaction to form willemite.

5. Conclusions

The conclusions are as follows.

(1) The activation energy of willemite formation was reduced from 228 to 167 kJ mol^{-1} by TiO_2 addition to the ZnO–SiO_2 powder mixture.

(2) TiO_2 addition to ZnO–SiO_2 melts retained the metastable phase, β-Zn_2SiO_4 to room temperature.

(3) The willemite of larger d-spacings and smaller c/a ratio obtained from β-Zn_2SiO_4 transformation was due to the partial incorporation of Ti^{+4} into Si^{+4} sites in the metastable β-Zn_2SiO_4.

Acknowledgements

Thanks are due to Institute of Earth Sciences, Academia Sinica, Republic of China for some X-ray and DTA analyses. This work was supported in part by National Science Council, Republic of China.

References

1. J. A. SPEER and P. H. RIBBE, in "Reviews in Mineralogy", Vol. 5, 2nd edn, edited by P. H. Ribbe (Mineralogical Society of America, Washington, D.C., 1982) p. 429.
2. F. H. NORTON, *J. Amer. Ceram. Soc.* **20** (1937) 217.
3. Z. STRNAD, "Glass Science and Technology", Vol. 8, (Elsevier, Amsterdam, 1986) p. 101 and literature cited herein.
4. E. N. BUNTING, *J. Amer. Ceram. Soc.* **13** (1930) 5.
5. A. E. RINGWOOD and A. MAJOR, *Nature* **215** (1967) 1367.
6. Y. SYONO and S. I. AKIMOTO, *J. Solid State Chem.* **3** (1971) 369.
7. A. SCHLEEDE and A. GRUHL, *Z. Elektrochem.* **29** (1923) 411.
8. J. WILLIAMSON and F. P. GLASSER, *Phys. Chem. Glasses,* **5** (1964) 52.
9. H. P. ROOKSBY and A. H. McKEAG, *Trans. Faraday Soc.* **3** (1941) 308.
10. H. F. W. TAYLOR, *Amer. Mineral.* **47** (1962) 932.
11. P. W. McMILLAN, G. PARTRIDGE and J. G. DARRANT, *Phys. Chem. Glasses,* **10** (1969) 153.
12. P. W. McMILLAN, "Glass Ceramics", 2nd edn (Academic Press, London, 1979) p. 76.
13. B. O. MYSEN, "Developments in Geochemistry", Vol. 4, (Elsevier, Amsterdam, 1988) p. 187.
14. F. H. DULIN and D. E. RASE, *J. Amer. Ceram. Soc.* **43** (1960) 130.
15. S. R. BARTRAM and R. A. SLEPETYS, *ibid.* **44** (1961) 493.
16. Y. HARADA and D. W. GATES, in "Ceramic Processing before Firing" edited by G. Y. Onoda, Jr. and L. L. Hench, (Wiley, New York, 1975) p. 449.
17. W. A. JOHNSON and R. F. MEHL, *Trans. AIME* **135** (1939) 416.
18. M. AVRAMI, *Chem. Phys.* **7** (1939) 1103.
19. *Idem., ibid.* **8** (1940) 212.
20. *Idem., ibid* **9** (1941) 177.
21. A. E. HOLLAND and E. R. SEGNIT, *Aust. J. Chem.* **19** (1966) 905.
22. B. K. VAINSHTEIN, V. M. FRIDKIN and V. L. INDENBOM, (eds), "Modern Crystallography, II, Structure of Crystals", (Springer, Berlin, 1982) p. 77.
23. S. F. HULBERT, *J. Brit. Ceram. Soc.* **6** (1969) 11.

Received 19 July
and accepted 22 November 1988